# PROCEEDINGS OF SPIE

SPIEDigitalLibrary.org/conference-proceedings-of-spie

Nonequilibrum phase transition in the light-actuated self-assembly of nanoparticles: effects of surfaces and stochastic forces

Ji, Haojie, Collison, Robert, Thomas, Daniel, Vuong, Luat

Haojie Ji, Robert Collison, Daniel Thomas, Luat T. Vuong, "Nonequilibrum phase transition in the light-actuated self-assembly of nanoparticles: effects of surfaces and stochastic forces," Proc. SPIE 11083, Optical Trapping and Optical Micromanipulation XVI, 1108325 (11 September 2019); doi: 10.1117/12.2528987



Event: SPIE Nanoscience + Engineering, 2019, San Diego, California, United States

# Nonequilibrum phase transition in the light-actuated self-assembly of nanoparticles: effects of surfaces and stochastic forces

Haojie Ji<sup>a</sup>, Robert Collison<sup>b</sup>, Daniel Thomas<sup>a</sup>, and Luat T. Vuong<sup>a,b,c</sup>

<sup>a</sup>Department of Physics, Queens College of the City University of New York, Flushing, NY
<sup>b</sup>Advanced Science Research Center, City University of New York, New York, NY
<sup>c</sup>Dept. of Mechanical Engineering, University of California at Riverside, Riverside, CA

#### **ABSTRACT**

When we illuminate gold nanofluids over indium-tin-oxide (ITO)-coated substrates, nanoparticle chains self-assemble via optical binding forces. We speculate that charge transfer between gold and ITO pins nanoparticles to the substrate and reduces the lateral Brownian motion as they attach to the substrate. We correspondingly model the self-assembly with additional stochastic or random forces. Simulations show a nonequilibrium-phase transition: when the stochastic force is small, nanoparticle chains align perpendicular to the light polarization and nanoparticles settle at shallow but stable nodes; when the stochastic force is large, however, the nanoparticle chains align parallel to the light polarization and nanoparticles settle at saddlepoints where the optical binding force is largely zero. Since the presence and strength of Brownian forces influence which state is formed, we reconsider the role that surfaces have—not only in relation to charge transfer but also heat transfer.

**Keywords:** plasmonic nanoparticles, light-induced self assembly, pattern formation, nonconservative mutual Lorentz force, nonequilibrium phase transition, stochastic forces, Brownian motion, plasmoelectric effect

# 1. INTRODUCTION

As nanotechnology rapidly develops, scientists are looking for new, low-cost ways to design nanostructures for large-area nanomanufacturing.<sup>1</sup> Colloidal self-assemblies represent some of the most promising bottom-up methods for building nanostructures over large areas, however there remain challenges in developing predictive approaches for anisotropic designs.<sup>2</sup> Some interesting large-area approaches include combined colloidal self-assembly with oscillation-evaporation dynamics of droplets,<sup>3</sup> surfactant modulation,<sup>4</sup> magnetic-field-driven and "patchy-particle" assembly.<sup>5</sup> Light-driven, top-down approaches in combination with bottom-up approaches have also drawn attention, since light can selectively actuate surface interactions at high speeds over large areas.<sup>6</sup>

We focus on understanding the self-assembly of metal nanoparticles (NPs), which is, at the very least, a process that is complicated in the presence of the plasmon excitation.<sup>7</sup> Their light-induced nanofluid mechanics depend on NP shape and geometry, and liquid solvent:<sup>8</sup> plasmons radiate<sup>9,10</sup> and produce heat,<sup>11</sup> which shift electrochemical potentials<sup>12</sup> that lead to movement,<sup>13</sup> which would further shift the plasmon excitation.<sup>14–16</sup> Our ability to predict and control the assembly of metal NPs in the presence of the plasmon excitation would advance the fields of nanomanufacturing and others associated with reconfigurable metamaterials.<sup>17</sup>

Plasmonic NPs self-assembly under the influence of the polarization-dependent optical binding force<sup>16</sup> and the optically-bound matter is held together by the interplay of driven states, i.e., plasmons. The colloidal structures held together by optical binding forces undergo dissipative, dynamic self-assembly,<sup>18</sup> which means that the system is in a steady state of nonequilibrium. Prior experiments with plasmonic NPs show the formation of predictable dissipative structures<sup>19</sup> and the disorder-to-order transition,<sup>20</sup> however in these environments, nanoparticles are illuminated at a wavelength red-shifted from the plasmon resonance.

Further author information: (Send correspondence to L.T.V.)

L.T.V.: E-mail: LuatV@UCR.edu

Optical Trapping and Optical Micromanipulation XVI, edited by Kishan Dholakia, Gabriel C. Spalding, Proc. of SPIE Vol. 11083, 1108325 ⋅ © 2019 SPIE CCC code: 0277-786X/19/\$21 ⋅ doi: 10.1117/12.2528987

In our prior work, we describe self-assembly from light illumination close to the plasmonic resonance of gold nanofluid droplets when dried on ITO-coated slides and we refer to the optical binding force as a mutual Lorentz force. The optical binding force arises from mutually-interacting plasmons and Lorentz forces, where surface charge and surface-charge motion couples to plasmon-radiated fields. We focus on an intermediate regime of NP concentrations where the self-assembly occurs, however this points to a trade-off and potentially problematic assumption: while NPs are expected to assemble if the optical binding force is "sufficiently large", when we increase the light intensity to increase the optical binding force, we heat the sample. Therefore, tuning the optical binding force changes the thermal and Brownian stochastic forces in the system, which influences the self-assembly.

Here, we describe recent efforts (both successful and unsuccessful) aligning gold NPs with light. We explore the predictability and reliability of the light-induced self assembly. Our prior efforts demonstrate polarization-dependent NP chains as long as  $200\mu$ m aligned perpendicular to the light polarization. Here, we provide evidence of electrostatic effects and charging of the substrate as the NPs attach to ITO, which could be explained by a plasmoelectric effect.<sup>12</sup> We also gain confidence in our model, which predicts the self-assembly from longitudinal dipole excitations (transverse-magnetic (TM) polarized light).

We also model the self-assembly and describe a phase transition, an ordered-state to ordered-state transition. We observe that when stochastic forces are small, then NP chains emerge perpendicular to the light polarization and NPs settle in stables nodes, or locations where the force points inwards. With larger stochastic forces, NP chains align with the linear polarization and NPs settle at locations where the optical binding force is zero. Our example is analogous to the sand and dust that separate and settle on nodes and antinodes of "Chladni plates". <sup>22</sup> Here, the critical parameter tuning the transition between these two regimes of the nonequilibrium-phase transition is the Brownian force.

#### 2. EXPERIMENT 1

#### 2.1 Method

Extending our prior work,<sup>21</sup> we study the lines formed by NPs in droplets as they dry under illumination of light. Stock gold NP solution (80-nm gold nanospheres, NanoXact 0.05 mg/mL, purchased from NanoComposix, PVP-coated 40 kDa (Polymer), 105-nm hydrodynamic diameter, -17-mV zeta potential, Milli-Q water solvent) is diluted with deionized distilled water to reach concentration 0.0375 mg/mL. A droplet is then dried on substrates of ITO-coated glass slides (IT100-111 purchased from NANOCS). While drying, the  $10-\mu$ L drop is illuminated by linearly polarized, 1.1-mm<sup>2</sup>, 532-nm wavelength,  $1-\mu$ J, 500-fs laser pulses at a 1-MHz repetition rate. The laser is defocused by a plano-convex lens so that the beam doubles in radius and covers the entire drop.

As shown in Fig. 1, here we consider oblique illumination and varied angles of the incident light polarization. We study the role of the longitudinal (z-direction) dipole oscillation or transverse-magnetic component of the light polarization. The incident laser is along the y-z plane. The incident angle ( $\theta_I$ ), the angle of the Poynting with substrate normal, varies from 0 to 60 degrees. The angle between the direction of linear polarization and the x-axis ( $\theta_P$ ) varies between 0 and 90 degrees with rotation of a zero-order half-wave plate in the optical path.

The dried samples are imaged with a scanning electron microscope (SEM). We observe self-assembled NP chains in the central region of the dried drops. The presence of the self-aligned patterns appear in regions of moderate NP area densities (6-16 NPs/ $\mu$ m<sup>2</sup>). The chains of NPs are generally aligned perpendicular to the direction of polarization of the laser. We ensure that the direction of the NP chains does not change with the orientation of the substrate. Hydrodynamic effects such as thermophoresis, evaporation, and convection are present, but are not expected to depend on light polarization, which is the focus of our analysis.

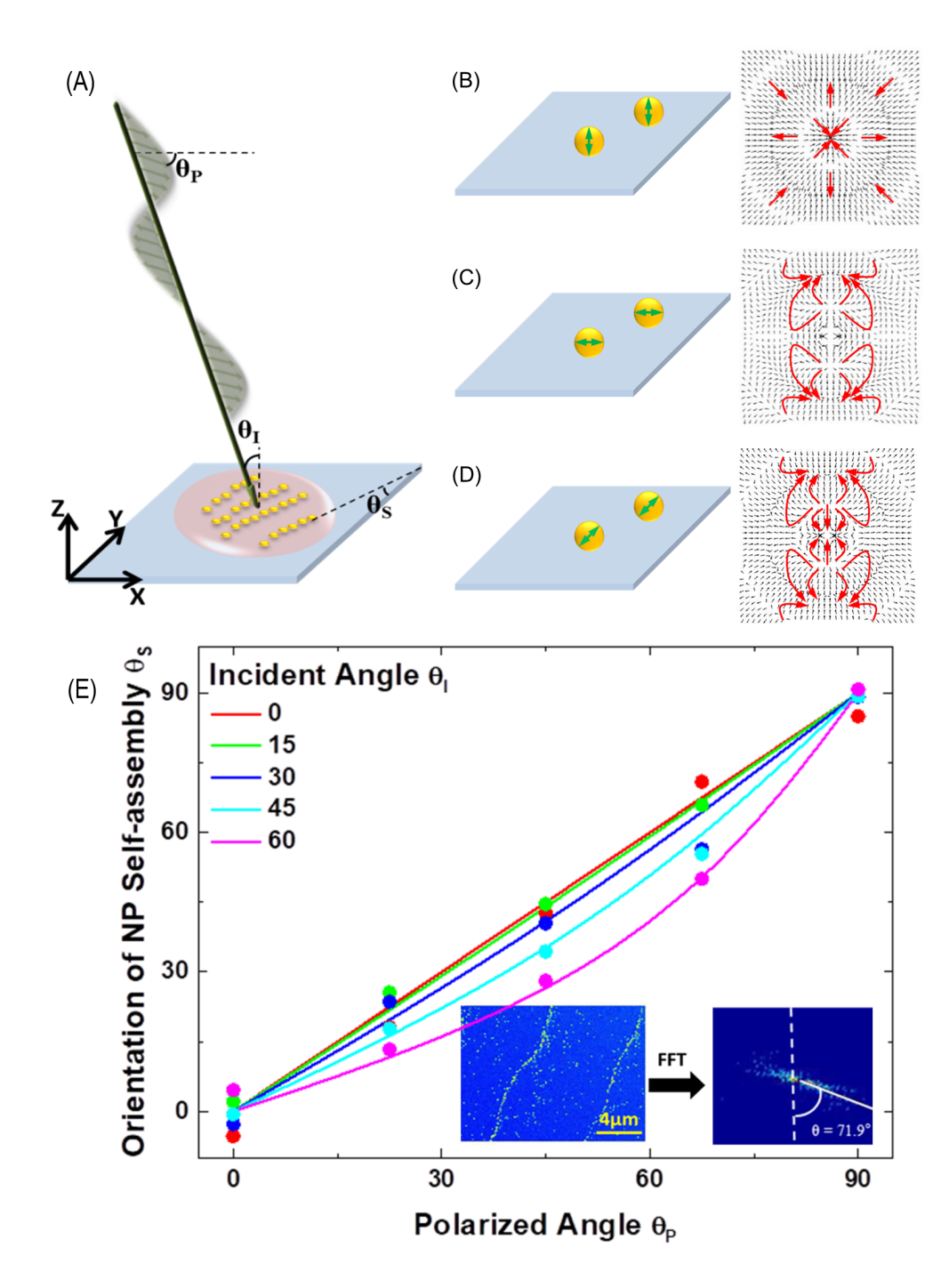


Figure 1. (A) Schematic diagram of the experimental setup and definition of angle parameters. Time-averaged force between dipoles oscillating (B) perpendicular to the substrate, where  $\theta_I = 90^{\circ}$  and  $\theta_P = 90^{\circ}$ , (C) along x-axis of the substract, where  $\theta_I = 0^{\circ}$ , and (D) 45 degrees above the plane of the substrate, where  $\theta_I = 45^{\circ}$  and  $\theta_P = 90^{\circ}$ . Arrows show the direction of the forces on a second NP in a 1500nm X 1500nm frame where of the first NP is fixed at the origin. The red lines represent the trajectory of the second NP. (E) The calculated (lines) and experimentally observed (dots) orientation of NP self-assembly (refer to y-axis of the SEM images) for various incident angle and polarized angle. Inset: SEM image and Fourier transform of the SEM image. The average and deviation of the NP chains is determined by the angle of the patterns in the Fourier domain.

#### 2.2 Observations

In general, the structure of the line patterns depends on the area density of the NPs, as reported in:<sup>21</sup> the NP area densities 6-16 NP/ $\mu$ m<sup>2</sup> produce the longest chains, generally >100  $\mu$ m. When the area density is higher, these longer NP strands appear more zigzagged. If the NP density is low (<1 NP/ $\mu$ m<sup>2</sup>), then the NPs are largely individually dispersed, and we infer that the separation between NPs results in Lorentz forces that are too small to overcome the randomly-directed forces associated with Brownian motion.

We speculate further on the role of the ITO coating, here. Strong solvent-substrate interactions are observed and are considered essential to the stability of the formed patterns. Previously, <sup>21</sup> we calculate the Brownian forces with dynamic light scattering measurements and surprisingly, the Brownian forces are at least an order of magnitude larger than the mutual Lorentz forces. Without an optical trap to confine NPs or surface pinning effects of the substrate, we expect that Brownian forces would arrest the long-range pattern formation associated with the optical binding force that we and others observe.

To explore the role of the substrate-NP interaction in the self-assembly, we prepare samples with which we block the laser two minutes before the solution drop is completely dry. As expected, we observe no NP chains in the majority of these samples; those chains that do form manifest to a much lower degree. Although this observation is not conclusive, we see that NP chains mostly connect during the last 1-2 minutes of drying when most NPs are close to the substrate.

Another indication that electrostatic interactions between the ITO-coated substrate and sample have a strong role in promoting self-assembly is that, where NPs aggregate into blocks or form thick lines, those NPs form a single mono-layer. Charge transfer between gold and ITO would lead to electrostatic forces that pin NPs to the ITO.<sup>12</sup> We generalize that the self-assembly occurs as follows. When NPs are close to the substrate, some NPs are pinned to the ITO, while others move in concert but experience reduced Brownian forces.<sup>23</sup> In regions of moderate NP density, the optical binding or mutual Lorentz forces overcome the Brownian motion. The assembling process commences after an initial group of NPs have been electrostatically pinned to the substrate. Initially NP chains are seeded by a dimer or a pair of attracted NPs. This pattern formation occurs in a manner analogous to spinodal decomposition and occurs uniformly throughout the sample, rather than at nucleation sites at the boundary of the sample.

# 2.3 Predictions

As shown in Fig.1 (A), we now consider oblique incidence of light to the substrate. The oscillating dipoles in this oblique illumination have both transverse and longitudinal contributions with respect to the substrate, and we now consider the force accompanying the 3rd, longitudinal dimension. The calculation of the mutual Lorentz force in the transverse direction due to the z-direction oscillation is shown in Fig. 1(B).

The time-averaged Lorentz force between a dipole oscillating in the z-direction and a dipole oscillating in the transverse plane is zero. Therefore, we separately consider the components of the time-averaged Lorentz force between z-oscillating dipoles [Fig. 1 (B)], and transverse or dipole oscillations in the x-y-plane [Fig. 1 (C-D)]. The z-components lead to radial, attractive or repelling forces depending only on the dipole separation. In contrast, the x or y-components lead to torques that turn the pair of NPs to align perpendicular to the dipoles.

For the laser with incident angle  $\theta_I$  and polarization angle  $\theta_P$  as defined in Fig. 1(A), the induced dipole p of each NP oscillates in the same direction as the laser field. We decompose the dipole into components normal  $p\cos\theta_P$  and parallel  $p\sin\theta_P$  to the incident plane. The dipole component parallel to the incident plane is decomposed into its vertical  $p\sin\theta_P\sin\theta_I$  and horizontal  $p\sin\theta_I\cos\theta_I$  components. Therefore, the dipole in the substrate plane has magnitude  $p\sqrt{\cos^2\theta_P + \sin^2\theta_I\cos^2\theta_I}$  and its direction is angled

$$\theta_S = \arctan(\tan \theta_P \cos \theta_I) \tag{1}$$

from the normal of the incident plane. Equation 1 is the angle between NP strings and the incident plane projected into the plane of the substrate. The presence of the z-direction dipole oscillation at larger angles of

incidence, will lead to a stronger isotropic attraction in the near field of the NPs (less than a half laser wavelength from the NP). In the near field, the force between z-component dipoles dominates, leading to a net attraction between the two NPs. At distances greater than half the laser wavelength from the NP, the forces between x-y dipoles dominate, which tend to align two NPs in a direction perpendicular to the oscillation or electric-field polarization. This explains why NPs align mostly perpendicular to the linear polarization even when light illuminates a surface at an oblique angle.

### 2.4 FFT Image Analysis

We analyze the images to consistently extract the orientation of the strings and understand the statistical variation of its alignment. We use the Fast Fourier Transform (FFT) in Matlab to obtain the frequency domain of the SEM images. Fourier analysis of the NP chains of the SEM images provides quantitative comparison of the images. The data from the FFT is then transformed into a Fourier image [Fig 1, (E)inset)]. The presence of unaligned NPs contribute to high-frequency noise or a halo in the FFT. We filter out the high-frequency halo to we find the region of points that represents the NP chains. The Fourier-space pattern direction is perpendicular to the alignment of NP chains in the original image. We take the average angle value of all of these filtered points and add 90° to determine the average angle of the NP chains in the SEM images.

We compare the experimentally extracted orientation of NP strings to the predicted values calculated from Eq. 1, plotted together in Fig. 1(E). Although standard deviations in the FFT-estimated angles are as much as 10 degrees, the NP string formation and alignment follows the relation calculated or Eq. 1.

For non-zero incident angles, the rotation of orientation of NP strings does not exactly match the rotation of laser polarization as it does for normally incident light. Indeed, as seen in Fig. 1(E), the angle between the NP string and the incident plane  $\theta_S$  is observed to be smaller than the angle between laser polarization and the normal of the incident plane  $\theta_P$ . The difference increases with increasing incident angle  $\theta_I$ . The angle of the projection of the horizontal component of the induced dipole varies less at larger angles of incidence. The contribution of the z-direction dipole component produces a force decreases  $\theta_S$ . This explanation agrees with our calculation.

The observed patterns change qualitatively as we increase the angle of incidence, as we would expect, indicating that the self-assembly (in spite of droplet Marangoni flows and thermoconvective dynamics) is predictable. As we increase the angle of incidence, the area of self-assembled pattern becomes smaller, and the average length of the NP strings gets shorter. The percentage of NPs involved in the string pattern formation decreases and meanwhile, more NPs are grouped into monolayer blocks. Increased reflection at increased angles of incidence and lower transmitted intensities are expected to explain the qualitative differences that result from reduced optical binding forces. In addition, an increased z-dipole oscillation promotes aggregation of NPs into clusters instead of lines [Fig 1(B)]. In other words, the z-dipole oscillation creates isotropic attraction between NPs, which tend to cluster into isotropic, block-like structures.

#### 3. CHALLENGES AND OUTLOOK

# 3.1 Experiments 2 and 3

The results from the Experiment 1 are promising, but unfortunately, when we aim to vary the polarization across the beam and manipulate the optical binding force, we experience only limited success. We illuminate the droplet with an azimuthally polarized vortex beam, which exhibits a singularity at its center where the intensity is strictly zero. As a result of the vortex profile, the light intensity is shifted across a larger area of the beam. Fig. 2(A) and (B) show SEM images consistent with what we observe in a donut region around the droplet. In this donut area, the NPs form individual lines that do not connect with others. The nonuniform spatial beam profile may influence the convection and we also expect that the light intensity may no longer be high enough over the larger, donut-shaped area of the droplet.

Additionally, we make an effort to pre-seed pattern formation, in order to produce more regular line patterns.

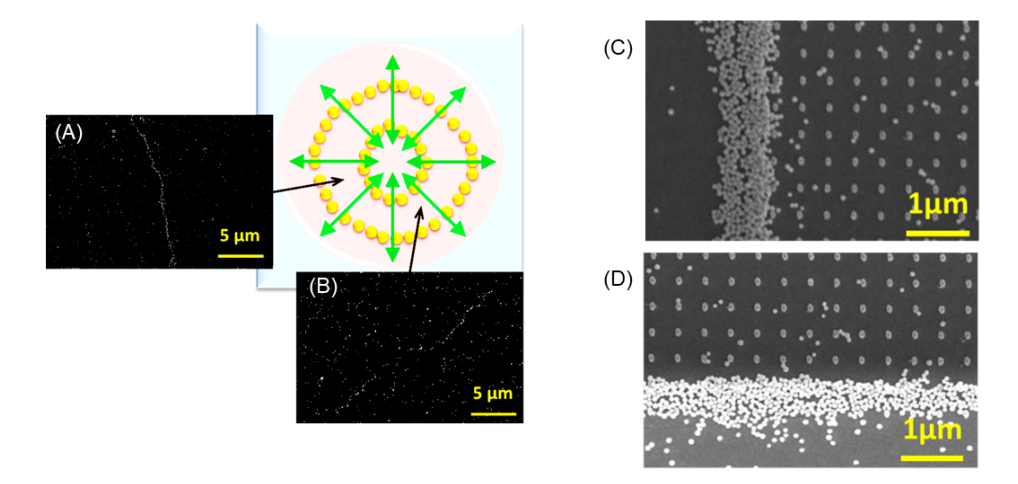


Figure 2. Background schematic shows the electric-field profile (green double arrows) created by vortex wave plate and the expected alignment of gold NPs. The insets show minimal success producing the expected alignment with SEM images taken from (A) the side and (B) bottom, as indicated by black arrows. In a separate experiment, we aim to seed pattern formation with a grid of NPs on the ITO substrate. SEM images show samples prepared on gold nanodisk array with gold NPs pushed to the (C) left and (D) bottom edges of the array.

We fabricate a grid of round nano-cylinders, which are intended to create a force profile that guides the NPs to form more consistent chains. For this purpose, we fabricated 2-D nano-cylinder array using electron-beam writing. The nano-cylinders are 80-nm diameter, 50-nm height, and 400-nm apart, as shown in Fig. 2(C) and (D). We subsequently dry the NP solution drop over the array while illuminating the drop with linearly polarized light, as before.

Unfortunately, we find that the NPs rarely settle inside the nano-cylinder array region and do not form string or network patterns. Instead, NPs prefer to attach to the edge of the array and form thick walls [Fig. 2(C-D)]. This effect warrants further study, and may be related to the thermal charging of the ITO coating close to the nano-cylinder grid associated with stronger light absorption and higher temperatures, or thermoconvective effects and thermophoresis. The enhanced gradient forces would also contribute to attraction at the edges: we calculate that the gradient forces at the edge of the grid to be twice that for an individual NP. Our trial efforts seeding pattern formation tell us that surface effects from the ITO substrate and potentially thermophoretic effect associated with the solvent close to the grid carry an outsized role in the self-assembly.

#### 3.2 Heuristic Modeling

We build a heuristic model based on the Green's function of the optical binding force between two particles.<sup>19</sup> The model includes gradient and scattering forces from other particles but assumes a uniform temperature distribution across the sample. We assume bulk nanofluid dynamics and plane-wave illumination. While local, near-field temperature gradients are not included, the effects of heating are included as a Brownian-motion parameter. We assume that dipoles are driven in phase and assume that the strength of the excitation does not change with time. At each step of the simulation, the program:

- Recalls each particle's position
- Applies periodic boundary conditions
- Calculates the force on each particle that depends on the relative position of every other particle
- Allows particles to move in the direction of the net force, in order of largest to smallest
- Repeats until particles find steady-state locations

What we learn from the simulations is that the final self-organized location of the NPs depends significantly on the Brownian motion parameter in the simulations, or the entropy of the system.<sup>20</sup> We observe in our simulations, as expected from our prior analysis, that the NPs both settle at stable nodes produced by the mutual Lorentz force where forces are pointed toward the same location. However, when the Brownian motion parameter is larger and the NP density is lower, NPs migrate towards locations where the force tends to zero. The transition is tuned with density of NPs and the Brownian motion parameter. In simulations, we observe NP lines to form both parallel and perpendicular to the linear polarization [Fig. 3].

Current simulations model 3D dipole oscillation dynamics in 2-D settling geometries, only. The prediction of the assemblies of 3-D assemblies in an optical trap and with fewer particles show hexagonal and rectangular lattices and are sufficiently different<sup>19</sup> that we suspect that the role of the optical trap carries a role. When the NP density is higher, near-field gradient forces and the interactions between the longitudinal component of dipoles lead to attraction between nearby NPs and the formation of connected chains turns into clusters of NPs, in a manner similar to that observed in experiments. The clusters are not consistently organized in a hexagonal or dimer lattice as others have predicted<sup>24,25</sup> but appear to be frustrated or locked in place. The heuristic simulations may bridge experimental observations.<sup>20,21</sup> Differences in the dynamics, likely related to trap illumination wavelength, intensity gradients, "entropy" or temperature, are worth considering further. The effect of the surfaces and surface interactions in relation to the Brownian motion<sup>23</sup> are expected to play an outsized role in optical-binding experiments.

#### 4. CONCLUSION

Some results aligning NPs on ITO substrate over large areas are reliable and promising, indicating that the alignment of nanoparticle chains associated with TM-polarization agree with our prior model and approach. The effects of electrostatic interactions with surfaces and the stochastic forces are still not clear.

Here, we focus on analyzing NP dynamics with unfocused light, close to the plasmonic resonance, and in the absence of an optical trap. Since the light-induced forces between particles are small in comparison to the convective and fluid dynamics in a droplet, we speculate that the electrostatic pinning of the NPs to the surface of ITO reduces Brownian motion and binds to other particles as they settle on the ITO surface. In other words, the presence of an ITO substrate appears to facilitate the formation of NP strings perpendicular to the linear light polarization.

We extend some prior efforts that illuminate challenges and demonstrate predictive control. We take SEM images of the self-assembled patterns over larger areas of the center of the dried droplets, sample and analyze the patterns to a greater degree, and demonstrate the role of the longitudinal dipole excitation. The dipole oscillation in the z-direction (perpendicular to the substrate) promotes aggregation. Our results indicate that our model is correct in spite of the complex interactions that are taking place in concert with the excitation of plasmons.

Further studies indicate that the degree of Brownian random motion carries an outsized role in the self assembly. In heuristic simulations, we observe a transition that occurs from perpendicular to parallel NP chain alignment with increased random motion, i.e., a heat-dependent nonlinear phase transition. Since the presence and strength of Brownian forces influence which state is formed, we reconsider the role that surfaces have—not only in relation to charge transfer but also heat transfer.

#### 5. ACKNOWLEDGMENTS

LTV acknowledges funding from NSF-DMR 1921034.

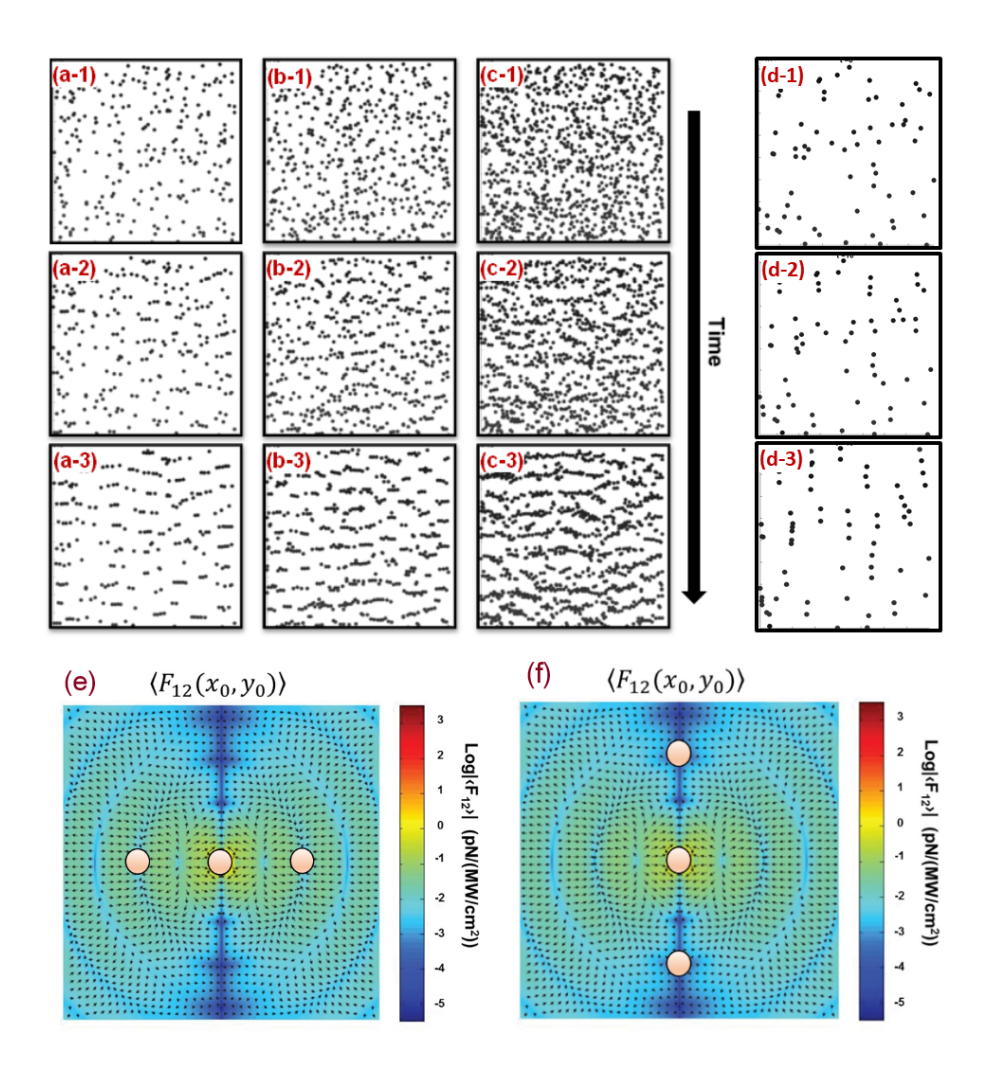


Figure 3. Simulation runs showing the evolution of NPs as a function of time for increasing concentration (a)-(c) and low entropy or temperature and (d) lower concentrations and higher entropy or temperature. Locations of 3 stable NPs where the NPs settle (e) where the net forces point towards, and (f) where the force magnitudes are largely zero, corresponding to low and high temperatures, respectively

#### REFERENCES

- [1] Liddle, J. A. and Gallatin, G. M., "Nanomanufacturing: A perspective," ACS Nano 10, 2995–3014 (Feb. 2016).
- [2] van Dommelen, R., Fanzio, P., and Sasso, L., "Surface self-assembly of colloidal crystals for micro- and nano-patterning," *Advances in Colloid and Interface Science* **251**, 97–114 (Jan. 2018).
- [3] Kabi, P., Chattopadhyay, B., Bhattacharyya, S., Chaudhuri, S., and Basu, S., "Evaporation-oscillation driven assembly: Microtailoring the spatial ordering of particles in sessile droplets," *Langmuir* **34**, 12642–12652 (Sept. 2018).
- [4] Morales, V. L., Parlange, J.-Y., Wu, M., Pérez-Reche, F. J., Zhang, W., Sang, W., and Steenhuis, T. S., "Surfactant-mediated control of colloid pattern assembly and attachment strength in evaporating droplets," *Langmuir* 29, 1831–1840 (Jan. 2013).
- [5] Zhang, J., Luijten, E., and Granick, S., "Toward design rules of directional janus colloidal assembly," *Annual Review of Physical Chemistry* **66**, 581–600 (Apr. 2015).
- [6] Fan, P., Zhong, M., Bai, B., Jin, G., and Zhang, H., "Large scale and cost effective generation of 3d self-supporting oxide nanowire architectures by a top-down and bottom-up combined approach," RSC Advances 6(51), 45923–45930 (2016).
- [7] Blattmann, M. and Rohrbach, A., "Plasmonic coupling dynamics of silver nanoparticles in an optical trap," *Nano Letters* **15**, 7816–7821 (Nov. 2015).
- [8] Dominguez-Juarez, J. L., Vallone, S., Lempel, A., Moocarme, M., Oh, J., Gafney, H. D., and Vuong, L. T., "Influence of solvent polarity on light-induced thermal cycles in plasmonic nanofluids," *Optica* 2, 447 (Apr. 2015).
- [9] Xu, H. and Käll, M., "Surface-plasmon-enhanced optical forces in silver nanoaggregates," *Physical Review Letters* **89** (Nov. 2002).
- [10] Haynes, C. L., McFarland, A. D., Zhao, L., Duyne, R. P. V., Schatz, G. C., Gunnarsson, L., Prikulis, J., Kasemo, B., and Käll, M., "Nanoparticle optics: the importance of radiative dipole coupling in two-dimensional nanoparticle arrays†," The Journal of Physical Chemistry B 107, 7337-7342 (July 2003).
- [11] Baffou, G., Quidant, R., and Girard, C., "Heat generation in plasmonic nanostructures: Influence of morphology," *Applied Physics Letters* **94**, 153109 (Apr. 2009).
- [12] Sheldon, M. T., van de Groep, J., Brown, A. M., Polman, A., and Atwater, H. A., "Plasmoelectric potentials in metal nanostructures," *Science* **346**, 828–831 (Oct. 2014).
- [13] Brooks, A. M., Sabrina, S., and Bishop, K. J. M., "Shape-directed dynamics of active colloids powered by induced-charge electrophoresis," *Proceedings of the National Academy of Sciences* **115**, E1090–E1099 (Jan. 2018).
- [14] Mirin, N. A., Bao, K., and Nordlander, P., "Fano resonances in plasmonic nanoparticle aggregates<sup>†</sup>," *The Journal of Physical Chemistry A* **113**, 4028–4034 (Apr. 2009).
- [15] Moocarme, M., Kusin, B., and Vuong, L. T., "Plasmon-induced lorentz forces of nanowire chiral hybrid modes," *Optical Materials Express* 4, 2355 (Oct. 2014).
- [16] Yan, Z., Sweet, J., Jureller, J. E., Guffey, M. J., Pelton, M., and Scherer, N. F., "Controlling the position and orientation of single silver nanowires on a surface using structured optical fields," *ACS Nano* 6, 8144–8155 (Aug. 2012).
- [17] Gardner, D. F., Evans, J. S., and Smalyukh, I. I., "Towards reconfigurable optical metamaterials: Colloidal nanoparticle self-assembly and self-alignment in liquid crystals," *Molecular Crystals and Liquid Crystals* **545**, 3/[1227]–21/[1245] (June 2011).
- [18] Fialkowski, M., Bishop, K. J. M., Klajn, R., Smoukov, S. K., Campbell, C. J., and Grzybowski, B. A., "Principles and implementations of dissipative (dynamic) self-assembly," *The Journal of Physical Chemistry B* 110, 2482–2496 (Feb. 2006).
- [19] Yan, Z., Shah, R. A., Chado, G., Gray, S. K., Pelton, M., and Scherer, N. F., "Guiding spatial arrangements of silver nanoparticles by optical binding interactions in shaped light fields," *ACS Nano* 7, 1790–1802 (Feb. 2013).

- [20] Nan, F., Han, F., Scherer, N. F., and Yan, Z., "Dissipative self-assembly of anisotropic nanoparticle chains with combined electrodynamic and electrostatic interactions," *Advanced Materials* **30**, 1803238 (Sept. 2018).
- [21] Ji, H., Trevino, J., Tu, R., Knapp, E., McQuade, J., Yurkiv, V., Mashayek, F., and Vuong, L. T., "Longrange self-assembly via the mutual lorentz force of plasmon radiation," *Nano Letters* 18, 2564–2570 (Mar. 2018).
- [22] Comer, J. R., Shepard, M. J., Henriksen, P. N., and Ramsier, R. D., "Chladni plates revisited," American Journal of Physics 72, 1345–1346 (Oct. 2004).
- [23] Jeney, S., Lukić, B., Kraus, J. A., Franosch, T., and Forró, L., "Anisotropic memory effects in confined colloidal diffusion," *Physical Review Letters* **100** (June 2008).
- [24] Tagliazucchi, M., Weiss, E. A., and Szleifer, I., "Dissipative self-assembly of particles interacting through time-oscillatory potentials," *Proceedings of the National Academy of Sciences* **111**, 9751–9756 (June 2014).
- [25] Helbing, D., Farkas, I. J., and Vicsek, T., "Freezing by heating in a driven mesoscopic system," *Physical Review Letters* 84, 1240–1243 (Feb. 2000).